Spectroscopic Study of Methinophosphide and Isocyanogen

by

Jianghong Wang

Submitted to the Department of Chemistry
in partial fulfillment of the requirements for the degree of

Master of Science in Chemistry

at the

MASSACHUSETTS INSTITUTE OF TECHNOLOGY

May 1994

Author .....
Department of Chemistry
May 20, 1994

Certified by .....
Robert W. Field
Professor of Chemistry
Thesis Supervisor

Accepted by .....
Glenn A. Berchtold
Chairman, Departmental Committee on Graduate Students

Spectroscopic Study of Methinophosphide and Isocyanogen

by

Jianghong Wang

Submitted to the Department of Chemistry
on May 20, 1994, in partial fulfillment of the
requirements for the degree of
Master of Science in Chemistry

Abstract

Unimolecular isomerization is a very important topic in molecular dynamics. We have studied the isomerization process of HCP $\leftrightarrow$ HPC by the technique of Stimulated Emission Pumping Spectroscopy. Highly vibrationally excited levels of Methinophosphide have been observed up to 25000cm^{-1}. Spectroscopic analysis has been attempted to understand the SEP spectrum. The observed spectrum shows some sign that isomerization might be beginning to occur at 25000cm^{-1} level. More experimental data is needed to fully understand the isomerization dynamics. We also propose an SEP experimental study of CNCN $\leftrightarrow$ NCCN utilizing a unique feature of the $(CN)_2$ isomers. Using the CNCN excited electronic state as the SEP intermediate, the energy barrier is reduced to 2/3 of the magnitude of that using the NCCN excited electronic state as SEP intermediate. *Ab initio* calculations confirm our prediction of the existence of a low-lying bent electronic state of CNCN. The proposed SEP experiments are therefore likely to succeed in characterizing the unimolecular isomerization of the CNCN $\rightarrow$ NCCN process.

Thesis Supervisor: Robert W. Field
Title: Professor of Chemistry

Acknowledgments

First of all, I want to thank my advisor, Bob Field for his guidance, advice and encouragement. From him, I learned about doing research in Physical Chemistry. Especially, I will always remember the tremendous support and understanding he gave me during my last year at MIT.

I also want to thank the former and present Field group members. I learned a lot from them and it has been an enjoyable experience for me.

I thank Wang Laboratory for the An Wang Scholarship and AFOSR for the financial support.

Finally, I want to thank my friends and family for their support and encouragement.

Contents

Chapter 1

Optical-Optical Double Reasonance Spectroscopy of Methinophosphide HCP

Isovalent to Hydrogren Cyanide, Methinophosphide (HCP) is a simple molecule which should be of great interest to many molecular spectroscopists. It is one of the few compounds in which a higher than second row element (P) is triply bound to a single carbon atom. The spectroscopic properties of HCP are very similar to those of HCN. Like HCN, the ultraviolet absorption spectrum is dominated by a bent $\tilde{A} \leftarrow$ linear $\tilde{X}$ transition. It is known that the bending potential of HCN has a local minimum which corresponds to the structure of HCN. Naturally one would be curious whether HCP has a similar structure on the ground state.

HCP was first synthesized by Gier [1] in 1964, who confirmed from the infrared spectrum that the molecule was linear with the structure of HCP rather than that of HPC. The excited electronic states of HCP were first observed by Johns *et al* [2] in 1969 using photographic UV absorption spectroscopy. They identified seven excited electronic states, including three singlet states: $\tilde{A}^1A''$ (T_0 = 34746 cm^{-1}), $\tilde{B}^1\Pi$ (T_0 = 35927 cm^{-1}), and $\tilde{C}^1A'$ (T_0 = 40248 cm^{-1}), and four triplet states: $\tilde{a}^3\Sigma^+$ (T_0 = 24440 cm^{-1}), $\tilde{b}^3\Pi$ (T_0 = 30430 cm^{-1}), $\tilde{c}^3\Sigma^-$ (T_0 = 31024 cm^{-1}), and $\tilde{d}^3\Pi$ (T_0 = 35976 cm^{-1}).

Of the seven observed electronic states, only $\tilde{A}^1A''$ and $\tilde{C}^1A'$ are bent, and this structural feature is crucial to the SEP experiments described later on. In 1989, *ab initio* configuration-interaction calculations by Karna *et al* [3] characterized several electronic states of HCP up to $65000cm^{-1}$. More *ab initio* calculations have been done on the ground state potential surface and the possible existence of HPC.

In 1982, Murrell *et al* predicted that HCP has a secondary energy minimum 367 kJ/mol above the minimum. However, their recent results [4] showed that HPC is a maximum. In 1985, Lehmann *et al* [5] showed in an *ab initio* calculation, that HCP has a saddle point on the ground state potential suffface corresponding to the structure of HPC. In addition, in a dispersed fluorescence spectrum from the $\tilde{A}$ state, they observed 94 vibrational states of $\tilde{X}^1\Sigma^+$ up to the energy of 17500 cm^{-1}. In 1986 from the results of *ab initio* MO studies, Nguyen *et al* [6] also suggested that HPC corresponds to an energy maximum and recently Ma *et al* [7] confirmed that HPC is a local energy maximum with respect to the bending coordinate and that HPC is indeed unstable in gas phase.

Our interest in the molecule is focused on the isomerization process of HCP $\Leftrightarrow$ HPC as studied by the technique of Stimulated Emission Pumping (SEP) Spectroscopy [8]. SEP is a two-laser experimental scheme. The first laser (PUMP) excites the molecule to a single rovibronic level of HCP in its excited electronic state. The seccond laser (DUMP) is scanned through resonance with downward transitions to the vibrationally excited levels of the ground electronic state. But the DUMP laser can also stimulate transitions upwards to higher excited states, as it did in our SEP experiments. This led to the observation of a previously unidentified electronic state.

The OODR experiments are carried out using a Nd:YAG laser which pumps two tunable dye lasers. The PUMP is a 15ns, 2mJ pulse (0.05 cm^{-1} resolution) of the frequency doubled output of a dye laser operated with an intracavity etalon. The PUMP transitions used in the OODR experiments were Q(6), P(7) lines of the $\tilde{A}^1A''$ $(0, 1^1, 0) \leftarrow \tilde{X}^1\Sigma^+$ $(0, 0^0, 0)$ band, Q(6), P(7) and Q(8) lines of the $\tilde{A}^1A''$ $(0, 0^0, 0) \leftarrow \tilde{X}^1\Sigma^+$ $(0, 1^1, 0)$ band, where $(v_1, v_2^{K_a}, v_3)$ are CH stretching, bending, CP stretching, and rotational angular momentum projection K_a along the **a** molecular

axis, respectively.

The $\tilde{A} \leftarrow \tilde{X}$ fluorescence was imaged by an S1UV lens onto the two matched end-on photomultipliers which monitor the signal and reference cells. Caution was taken to minimize the scattered light. The output of the PMT signal was amplified by a LeCroy VV100BTB amplifier and sent to a home-built differential amplifier. The output of the differential amplifier was detected by a SRS 250 boxcar. The boxcar settings usually are: width $1.5\mu s$, delay 100 - 200 ns, averaged shots 30. The PUMP laser was pressure-scanned and locked onto a specific rotational transition. The PROBE laser is a 5 mJ pulse, delayed with respect to the PUMP by 20 ns. By counter-propagating the PUMP pulse only through the singal cell, the PROBE laser excited the $3^1A' \leftarrow \tilde{A}^1A''$ $(0, 1^1, 0)$ transition.

The OODR signal was detected by the depletion of the side fluorescence in the signal cell as the PROBE laser was scanned through resonance with an upward transition. The PROBE laser covered the region from 49000 cm^{-1} to 56000 cm^{-1}. Most of the OODR spectra were recorded with a resolution of $0.5cm^{-1}$ by grating-scanning the PROBE laser. The (0, 0, 0) and (0, 1, 0) vibrational levels of the $3^1A'$ state were recorded at 0.05 cm^{-1} resolution by pressure-scanning the PROBE laser with an intracavity etalon and calibrating against the I_2 atlas. Both the PUMP and the PROBE lasers were linearly polarized with their polarization axe parallel with each other.

The HCP sample was synthesized by pyrolysis of CH_3PCl_2 [9] at $\sim 900°C$ in a 30 cm long, 7 mm diameter quartz tube packed with crushed quartz. The gaseous products were passed through a KOH trap at 200 K, which removed HCl and low volatility products. A second trap at 77 K collected HCP product and passed CH_4 product and other low boiling products. HCP along with some C_2H_2 byproduct was evaporated from the second trap at 130 K. Since we were using a double resonance technique, no attempt was needed to separate C_2H_2 from HCP. The sample pressure inside the cell was usually around 300 mTorr.

Contrary in appearance to the usually sharp (FWHM = 0.05 cm^{-1}) features of the SEP spectra, the spectral linewidth of each OODR features is much broader. This

made it easy to distinguish the upward OODR transitions from the downward SEP transitions. We could also compare the observed Q(6) and Q(7) PUMPed spectra which would include transitions into the same $J'' = 6$ and 7 levels of the $3^1\tilde{A}'$ state. If the transition is upward, the Q(7)-PUMPed spectrum is going to be shifted to a higher frequency by $J'' * (B' + C')$ cm^{-1}. On the other hand, if the Q(7) spectrum had to be shifted to lower frequency by roughly the same $J'' * (B' + C')$ cm^{-1} to bring it into overlap with the Q(6) PUMPed spectrum, the transition must be a downward SEP signal. So with these two methods, we can definitely distinguish downward SEP transitions from upward OODR transitions.

The newly observed electronic state of HCP is assigned to be a bent singlet state with the $^1A'$ symmetry. The calculation by Karna [3] suggests that this is the third state of A' symmetry, hence it is called $3^1A'$. It corresponds to two $\pi^* \leftarrow \pi$ excitations, since the $3^1A'$ and the $X^1\Sigma^+$ ground state belong to the electronic configurations: $(1\sigma - 7\sigma)^2(1\pi)^4(2\pi)^2(3\pi)^2$ and $(1\sigma - 7\sigma)^2(1\pi)^4(2\pi)^4$ respectively. From the priliminary analysis of the OODR spectra, we believe that the predissociated bent $3^1A'$ state is a quasilinear state, which means that the barrier between the bent equilibrium configuration to the linear configuration is very shallow, comparable to the energy of several quanta of the bending vibrational excitation. So the molecule can easily surmount the barrier and display the effects of a transition from bent to linear geometry. Therefore, the spectrum of a bending vibrational progression will have similar structure of the bent to linear transition, usually in the form of a rapid increase of the A rotational constant and decrease of the vibrational interval as v_{bend} increases.

Chapter 2

Least-Square Fitting of the SEP Spectrum of Methinophosphide HCP

2.1 Introduction

Since the Herzberg era of molecular spectroscopy, experiments on polyatomic molecules have been limited to the study of a few vibrational quanta, where the energy is localized in certain normal modes. But at vibrational energies of chemical interest, spectroscopists encounter enormous difficulties both experimentally and theoretically. The first is the difficulty of the experiment itself. For example, the intensity of vibrational overtone bands, whereby a molecule is excited directly to a high vibrational overtone level, will decrease by roughly a factor of 10 each time the vibrational excitation increases by 1. For the HCP molecule, the isomerization barrier of HCP $\leftrightarrow$ HPC is estimated to be $\sim 27000 cm^{-1}$ by recent *ab initio* calculation [10], which corresponds to approximately 45 quanta of the bending vibration. So there is no way this barrier maximum region can be reached by the method of direct overtone pumping. The second problem is spectral congestion. When the vibrational excitation reaches $v >> 1$, the vibrational density of states can be as high as $10/\text{cm}^{-1}$ and it will be extremely hard to resolve and even more difficult to assign the spectrum. On the

theoretical side, normal mode analysis has been well understood since the 1950's, but it is limited to the approximation of small-amplitude motion. Can the normal mode theory be extrapolated to energy levels up to tens of quanta of vibrational excitation where molecules exhibit large amplitude motions? How can the spectra of highly vibrationally excited molecules be understood? What information about the molecular dynamics can be extracted from the spectra? These are serious challenges for molecular spectroscopists.

In 1979, Field, Kinsey and coworkers invented the technique of Stimulated Emission Pumping Spectroscopy (SEP) [8]. SEP is a folded variant of Optical-Optical Double Resonance Spectroscopy and has been proved to be extermely valuable in exploring the dynamics of highly vibrationally excited molecules, such as HCCH, HCN, etc. The first laser (PUMP) stimulates transitions to a selected rovibronic level of a well-characterized excited electronic state, then the second laser (DUMP) stimulates transitions back to the ground electronic state potential surface. When the DUMP laser is tuned to resonance with a transition into high vibrational levels of the ground state, stimulated emission occurs and the SEP signal corresponds to a fluorescence dip resulting from each the DUMP resonance. The double resonance feature of SEP greatly reduces the spectral congestion. SEP is also a Franck-Condon selective technique which makes the spectra much easier to asssign. One thing to notice is that, even with the advantages of SEP, it is fairly difficult to analyse the spectra of highly vibrationally excited levels in practice due to various anharmonic and Coriolis interactions. The crucial condition in an SEP experiment is the structural and dynamical characteristics of the intermediate electronic state, such as its lifetime, fluorescence yield, dissociation limit. An other condition is the equilibrium geometry of the intermediate state which determines the Franck-Condon overlap integral between the intermediate and the final state. The overlap integral directly controls the transition intensity.

2.2 Overview of the SEP Data Set of HCP

The SEP experiments on HCP were similar to the description of the OODR experiments and details can be found in many references [11]. The only difference between an OODR experiment and an SEP experiment is that the second laser (DUMP) stimulates transitions from the intermediate state back to the highly vibrationally excited levels of the ground electronic state. Usually SEP spectra were recorded in high resolution (0.05 cm^{-1}) by pressure-scanning the DUMP laser with an intracavity etalon.

Since one can think of the bending vibration of HCP as the isomerization coordinate, the SEP experiments concentrated mainly on the pure bending overtones. The intermediate states used in the SEP experiments of HCP were the bent $\tilde{A}^1A''$ and $\tilde{C}^1A'$ states and the specific intermediate vibrational levels were selected to get optimal Franck-Condon overlaps. The $\tilde{A} \leftarrow \tilde{X}$ transition is a parallel c-type transition with the rotational rule of $K' - l'' = \pm 1$. If the PUMP transition was HCP $\tilde{A}^1A''$ $(0, 3^1, 0) \leftarrow \tilde{X}^1\Sigma^+$ $(0, 0^0, 0)$ which means that $K'_a = 1$, we would expect that the terminal levels of the SEP spectrum will have even quanta of the vibrational angular momentum l''. This implied that only vibrational states with even quanta of bending excitation would be reached in the SEP spectra. On the other hand, if the PUMP is a hot band transition, such as $\tilde{A}^1A''$ $(0, 3^0, 0) \leftarrow \tilde{X}^1\Sigma^+$ $(0, 1^1, 0)$, then odd quanta of the bending vibration would be reached in the SEP spectra. This provides preliminary assignments of the vibrational sequences of the SEP spectra.

Basically, the SEP experiments began with the (0, 26, 0) state at 16318 cm^{-1} stimulated by the results of Dispersed-Fluorescence spectroscopy reported by Lehmann *et al* [5]. The pure bending overtones were observed from (0, 26, 0) up to (0, v_2, 0), v_2 = 26, 28, 30, 32, 34, 36, 38, 40, 42. For the (0, 42, 0) state, the vibrational energy is around 25315 cm^{-1}, which is close to the top of the HCP $\leftrightarrow$ HPC isomerization barrier, 27000 cm^{-1}. Two combination levels with CP stretch were also observed, (0, 24, 1) and (0, 26, 1).

One interesting observation is the pattern of Franck-Condon selectivity of the

intermediate levels of the $\tilde{A}$ state. From the $\tilde{A}^1A''$ state (0, 3, 0) level, the highest observed states were (0, v_2, 0), where $v_2 \leq 30$. While for the (0, 3, 1) level, only two states were observed, (0, v_2, 1), where $v_2 = 24, 26$. For the $\tilde{A}$ (0, 3, 3) level, we were able to observe levels as high as (0, 42, 0). On the other hand, if the $\tilde{C}$ state was the intermediate level, no Franck-Condon selectivity was apparent and the observed density of states was equal to the calculated density of states. What role did the excitation of the CP stretch of the $\tilde{A}$ state play in the SEP spectrum and what is the reason for such a distinct pattern of Franck-Condon selectivity for the $\tilde{A}$ state?

The bending overtone spectra showed no perturbations up to $v_2 = 30$, which is very surprising since the energy is about 19000 cm^{-1} at $v_2 = 30$. But at $v_2 = 32$, the spectrum was observed to be heavily perturbed and the perturbations were not as strong and numerous for states of $v_2 > 32$ than for $v_2 = 32$. This is very weird since usually the intensity and complexity of perturbations increase monotonically with the vibrational excitation. The sudden onset of perturbations at the (0, 32, 0) level itself is intriguing, but it is also hard to understand is why the perturbations are less numerous and intense at (0, $v_2 > 32$, 0) than at (0, 32, 0).

From the Franck-Condon principle, the CP stretch should be active in the $\tilde{A} \leftarrow \tilde{X}$ transition since the CP bond length changes from 1.54 Å in the $\tilde{X}$ state to 1.69 Å in the $\tilde{A}$ state. But we only saw two SEP transitions into states with excitation in the CP stretch. All other combination levels which would be expected to occur in the examined energy region were not seen. Due to the Franck-Condon selectivity of the $\tilde{A}$ state, one might think that the combination levels do not have overlap with the $\tilde{A}$ state wavefunction.

2.3 Least-Squares Fitting

For each bending overtone state, the number of actually observed perturbing vibrational states ranges from 1 to 10. The objective of doing Least-Squares Fitting is to deperturb the observed SEP spectra and understand the resonances among all the observed states. If possible, we want to see whether there were any signs of

isomerization since the highest reached energy was very close to the calculated isomerization barrier. We used a Nonlinear Least-Square Fitting program [12] developed in this group. Basically, we write down the effective Hamiltonian matrix for the observed group of states, which consists of the Franck-Condon bright state (a bending overtone) and the Franck-Condon dark states, which showed up in the SEP spectra through spectroscopic perturbations. The computer diagonizes the matrix to determine the eigenvalues, which are supposed to correspond to the observed molecular energy levels.

2.3.1 Basis Function

The vibrational wavefunction of the linear ground state of HCP is labelled: (v_1, v_2^l, v_3), where v_1, v_2, v_3 are CH stretch, bend, CP stretch respectively, and l is the vibrational angular momentum arising from the doubly degenerate bending vibration. The transformation for the $\tilde{X}$ state vibrational wavefunction under σ_v, reflection in the molecule fixed plane, where the reflection symmetry corresponds to the parity is:

$$\sigma_v|v_1, v_2^l, v_3 >= |v_1, v_2^{-l}, v_3 >.$$

The $\tilde{X}$ state rotational wavefunctions were expressed in the parity basis, $|J, l, e >$ and $|J, l, f >$, which can be expressed as linear combination of the signed-l basis functions:

$$|J, l = 0e >= |J, l = 0 >$$

$$|J, l = 2, e >= \frac{1}{\sqrt{2}}(|J, l = 2 > + |J, l = -2 >)$$

$$|J, l = 2, f >= \frac{1}{\sqrt{2}}(|J, l = 2 > - |J, l = -2 >),$$

where J is the total angular momentum, l is the vibrational angular momentum. Note that, for a linear molecule, l is the same as K_a, the projection of J on the **a** molecular axis. For the linear HCP ground state, l is used instead of K hereafter.

We know that in the signed-l basis:

$\sigma_v|J,l>=(-1)^{J-l}|J,-l>$.

It is easy to work out in the *e, f*-symmetry basis that:

$\sigma_v|J,l,e>=(-1)^{J}|J,l,e>$

$\sigma_v|J,l,f>=(-1)^{J+1}|J,l,f>$.

The advantage of using the *e, f*-symmetry basis is that the perturbation selection rules are easy to define in the *e, f*-symmetry wavefunction and the off-diagonal matrix elements will be easy to write down.

2.3.2 Matrix Elements

The diagonal matrix elements used here are just standard energy level expressions for a linear triatomic molecule:

$$E=\nu_0+g_{ll}l^2+B_v(J(J+1)-l^2)-D(J(J+1)-l^2)^2 \tag{2.1}$$

The off-diagonal matrix elements can have various forms depending on the type of interaction between each state. The frequently used types of interactions are described in the following.

a) **Rotational l-type resonance** is the interaction between the $l=0$ and $l=2e$ parity component of the same vibrational state. It is the most important interaction between the $l=0e$ and $l=2e$ parity states of the Franck-Condon bright states. As a second-order effect of the Coriolis interaction [13], the rotational l-type resonance has the following matrix element in the signed-l basis:

$<v_1,v_2^l,v_3;J,l|H|v_1,v_2^{l\pm2},v_3;J,l>=$

$\frac{1}{4}q_2\sqrt{(v_2\mp l)(v_2\pm l+2)[J(J+1)-l(l\pm1)][J(J+1)-(l\pm1)(l\pm2)]}$.

In the parity basis, it can be shown that the matrix elements between the $l=0$

and $l = 2e$ parity component is:

$$V_{l-res} = \frac{\sqrt{2}}{4} q_2 \sqrt{v_2(v_2+2)J(J+2)[J(J+2)-2]} \tag{2.2}$$

b) **Fermi Resonance** [14] is caused by the third order anharmonicity of the potential energy surface. It occurs whenever the sum of the frequencies of $\omega_i + \omega_j$ (or $2\omega_i$) is accidentally close to the frequency ω_k and the cubic force constant k_{ijk} (or k_{iik}) does not vanish by symmetry. For the linear HCP molecule, no Fermi resonance has been reported in the microwave and infrared data. From the consideration of symmetry and vibrational frequencies, operators of the form $r_2^2 q_3$, where r_2 is the radial bending normal coordinate and q_3 is the "CP" stretch mormal coordinate, lead to a 2:1 bend:"CP" stretch resonance. The matrix element for the 2:1 resonance can be expressed as the following:

$$\begin{aligned} &< v_1, v_2^l, v_3 | H | v_1, (v_2-2)^l, v_3+1 > \\ &= k_{0:2:1} \sqrt{(v_2^2 - l^2)((v_2-2)^2 - l^2) v_3 (v_3+1)} \end{aligned} \tag{2.3}$$

where $k_{0:2:1}$ is the force constant coefficient of the $r_2^2 q_3$ term of the potential energy. Note that the Fermi interaction exists only between states with the same value of l and its magnitude does not depend on the rotational quantum number J, but it increases with the vibrational quantum numbers to specific powers. This is a very useful type of information for assigning the the perturber states. In the actual fit, the matrix elements will simply be assumed to be constant between each pair of interacting states.

c) **Coriolis Interaction** [14] is caused by the coupling of the total angular momentum J and the vibrational angular momentum π. The Coriolis term in the Hamiltonian for a linear molecule is: $(J \times \pi)_z$. The corresponding matrix elements in the signed-l basis are:

$$< v_1, v_2^l, v_3; J, l | H | v_1, (v_2 \pm 1)^{l \mp 1}, v_3 + 1; J, l \pm 1 >$$
$$= \xi \sqrt{J(J+1) - l(l \mp 1)} \sqrt{v_1 (v_2 \pm 1)(v_3 + 1)} \text{ where } \xi \text{ is a con-}$$

stant which depeds on the normal coordinates. This a-type Coriolis interaction connects states with $\Delta l = \pm 1$ and the interaction gets stronger as the rotational quantum number J increases. So one would expect that, if there is a Coriolis interaction between two states, the matrix elements will get larger as J increases. In the fit, the Coriolis matrix elements in the parity basis are taken to be:

$$V_{Coriolis} = C_v \sqrt{J(J+1) - l(l+1)} \tag{2.4}$$

where l is that for the Franck-Condon bright state, and C_v is vibrational-dependent constant.

2.4 (0, 32, 0) State

The PUMP transitions used for the (0, 32, 0) state were Q branch lines of the $\tilde{A}(0, 3^1, 1)$ band, $J = 3, 4, 7, 8, 13$ and Q branch lines of $\tilde{A}(0, 4^1, 1)$ band, $J = 4, 6, 7, 8$.

The (0, 32, 0) state is the most strongly perturbed state of the observed bending overtones. Even simplifed by SEP, the observed spectrum is very complicated. One thing to notice is that the number of observed lines increases with respect to J, which indicates that the off-diagonal matrix elements between the bright (0, 32, 0) state and the highly excited vibrational perturber states are J-dependent. Only one Franck-Condon bright state was considered and the spectroscopic constants are listed in Table 2.3 at the end of this chapter. We tried to use an effective Hamiltonian model to fit the observed data but were unsuccessful.

2.5 (0, 34, 0) State

The PUMP transitions used for (0, 34, 0) states were: Q branch lines of the $\tilde{A}(0, 3^1, 2)$ band, $J = 7, 8, 9, 12$ and Q branch lines of the $\tilde{A}(0, 4^1, 1)$ band, $J = 6, 7, 12, 13, 14$. Basically, the observed spectra consisted of three vibrational states: the (0, 34, 0) F-C bright state ($l = 0$ and 2), and two extra states labelled * and ** as shown in the reduced term value plots. Note that the * and ** states have e symmetry because the

two states only appeared in the Q PUMP and Q DUMP spectra. In the symmetry basis, the total selection rule is: $e \leftrightarrow f$ for Q type transitions and $e \leftrightarrow e$ for P and R type transitions. So it's straightforward to confirm that after two consective Q type transitions, the terminal states will have the same parity as the initial state. In our case, the initial ground state has e parity, so the terminal states also must have e symmetry.

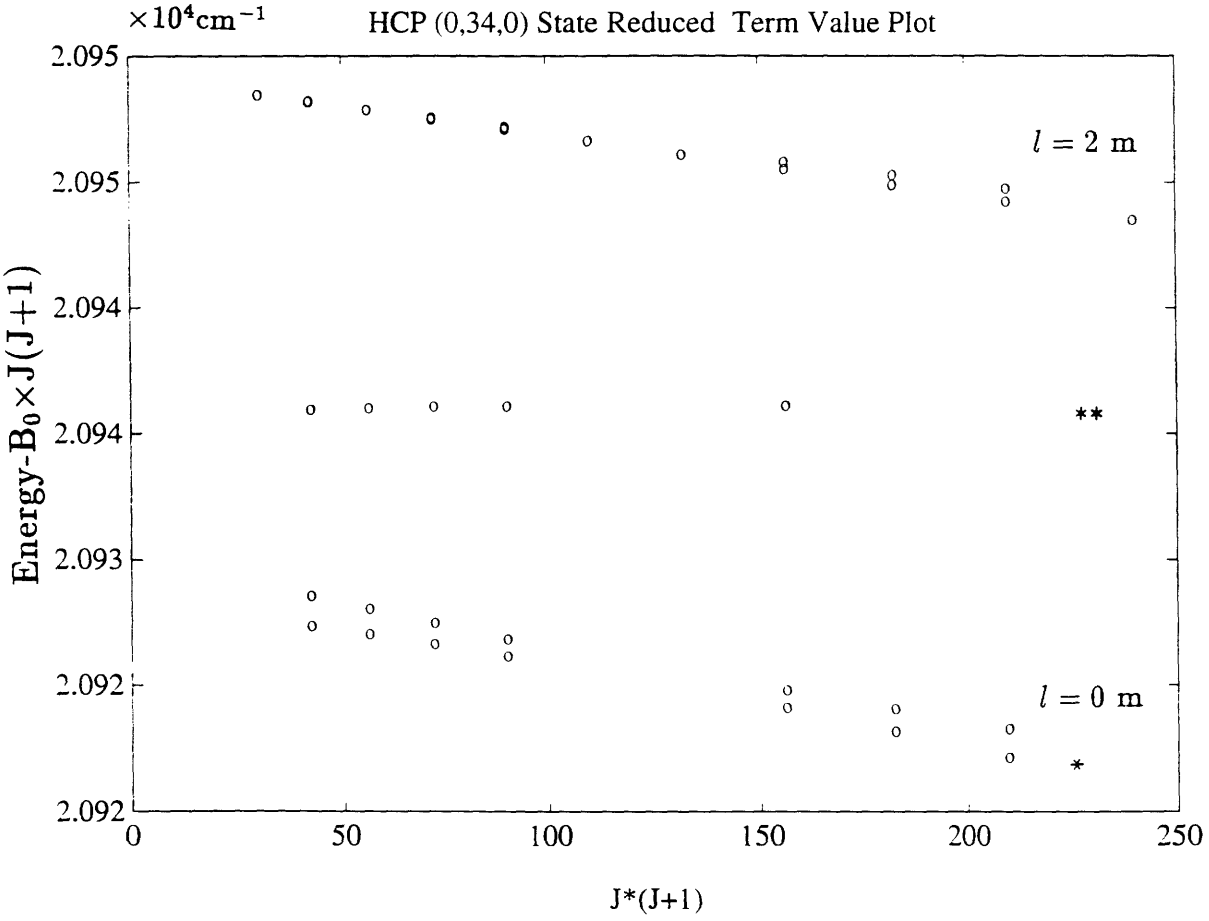

Figure 2.1 HCP (0,34,0) state reduced term value plot.
B_0=0.6662735 cm^{-1}.

We can write down the effective Hamiltonian matrix:

$$\begin{pmatrix} H_m^{l=0} & H_{l-res} & H_{13} & H_{14} & 0 \\ H_{l-res} & H_m^{l=2e} & H_{23} & H_{24} & 0 \\ H_{31} & H_{32} & H_* & 0 & 0 \\ H_{41} & H_{42} & 0 & H_{**} & 0 \\ 0 & 0 & 0 & 0 & H_m^{l=2f} \end{pmatrix} \qquad (H_{ij} = H_{ji}) \qquad (2.5)$$

The diagonal terms are the standard zero-order rovibrational energy level expressions for a linear triatomic molecule, as in equation (2.1). There are no off-diagonal matrix elements between the e parity block and the f parity block due to reflection symmetry, and all interactions between the Franck-Condon dark states are also assumed to be 0. There is an l-resonance of the form of Equation (2.2) between the $l = 0$ and $l = 2$ e parity components of the main state. The interactions between the main state and the * are assumed to be different types of mechanisms such as Coriolis and Fermi and the interaction between the main state and the ** state are also assumed to be either Fermi or Coriolis.

The crucial goal here is the l assignment of the * and ** states. If $l = 0$ for both states, only Fermi resonance is plausible and we obtain:$H_{13} = F_1$, $H_{14} = F_2$ and $H_{23} = H_{24} = 0$. If $l = 1$, the interaction takes the Coriolis form and we have: $H_{1i} = C_i\sqrt{J(J+1)}$ and $H_{2i} = \frac{1}{\sqrt{2}}C_i\sqrt{J(J+1)-2}$, where $i = 3, 4$ indicating the * and ** states. The factor of $\frac{1}{\sqrt{2}}$ comes from the fact that the $l = 2, e$ parity level is a linear combination of two signed-l basis functions with a normalization constant of $\frac{1}{\sqrt{2}}$. Finally, since the * and ** states only showed up in the spectra as single e parity components, these perturbers cannot be $l = 2$ states.

We tried different combinations of the above mechanisms and the result showed that the interaction between * and (0, 34, 0) is Coriolis type, i.e. $l^* = 1$, and that between ** and (0, 34, 0) is Fermi type, i.e. $l^{**} = 0$. The fit was very good and the differences between the experimental data and the calculated energy levels were well within the experimental error of 0.05 cm^{-1} for all observed rotational lines. Moreover,

the experiments on the J-dependence of the intenstiy ratios between the * state and (0, 34, 0) confirmed that the interaction strength was rotation-dependent since the intensity ratio of the * state relative to the (0, 34, 0) state was increasing with J and in good agreement with the the calculated ratio calculated for the Coriolis interaction. So we concluded that the * state was an $l = 1$ state with a Coriolis interaction with the (0, 34^0, 0) state and the ** state was an $l = 0$ state with a Fermi resonance interaction with the (0, 34^0, 0) state. The matrix elements between the (0, 34, 0) state and the *, ** states were determined to be: $0.02862\sqrt{J(J+1)}$ cm^{-1} and 0.5 cm^{-1} respectively. The spectroscopic constants for the * and ** states are listed in Table 2.1.

	ν_0 (cm^{-1})	B_v (cm^{-1})
*($l = 1$)	20930.29(77)	0.6236(11)
**($l = 0$)	20935.67(9)	0.6721(1)

Table 2.1. Spectroscopic Constants of the purturbed states of (0, 34, 0), (1σ uncertainties in parentheses).

2.6 (0, 36, 0) State

The PUMP transitions used for the (0, 36, 0) state were the Q branch lines of the $\tilde{A}(0, 3^1, 2)$ band, $J = 6, 7, 8, 11, 12, 13$. In the reduced term value plot, we can see that there were 3 vibrational states: the FC bright (0, 36, 0) state and two extra * and ** states similar to (0, 34, 0). Chen *et al* [15] assigned the two extra states to be $l = 0$ states and the fit was excellent.

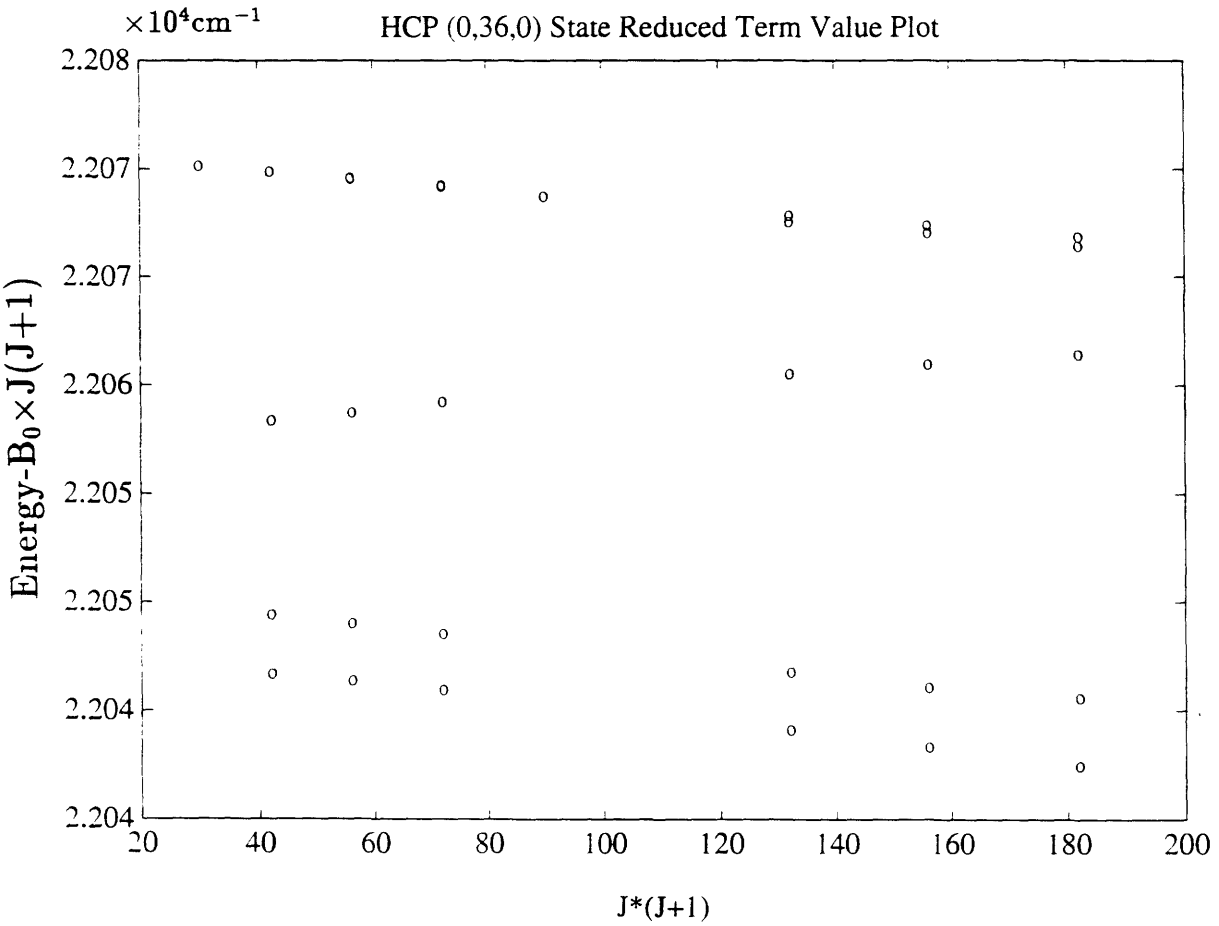

Figure 2.2 HCP (0,36,0) state reduced term value plot.
B_0=0.6662735 cm^{-1}.

2.7 (0, 38, 0) State

The PUMP transitions used for (0, 38, 0) state were Q branch lines of the $\tilde{A}(0, 3^1, 3)$ band, $J = 1, 2, 3, 4, 6, 7, 8, 9, 10, 11, 12, 13$. The number of observed states is larger than those for the (0, 34, 0) and (0, 36, 0) states, but smaller than those for (0, 32, 0).

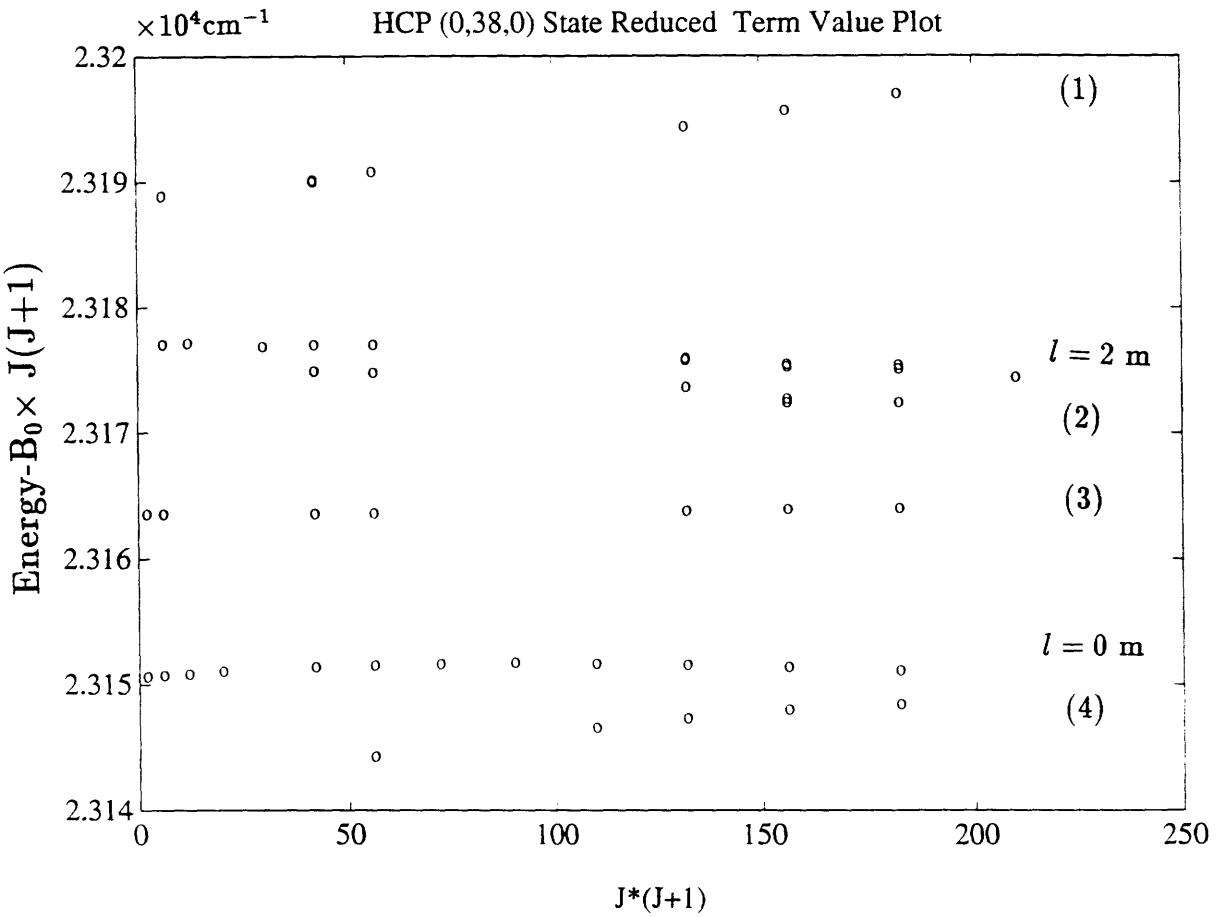

Figure 2.3 HCP (0,38,0) state reduced term value plot.
B_0=0.6662735 cm^{-1}.

As shown in the reduced term value plot, we identified 6 vibrational states from the spectra. The Franck-Condon bright states are: $l = 0$ and 2 (0, 38, 0) states for which assignments are made confidently from the expected term value and the relative intensity. The others are, in descending energy order, 1) $l = 1$ or 2 state, 2) $l = 1$ or 2 state, 3) $l = 0$ state, 4) $l = 0$ state. The l assignments were based on the following observations: states 3) and 4) only showed up in the Q-PUMP and Q-DUMP spectra, and this confirmed that these states are definitely $l = 0$ e parity states. Otherwise we would expect to observe double parity states due to the transition selection rule of $\Delta J = \pm 0, 1$. On the other hand, states 1) and 2) were indeed observed for both e and f parities. But whether these states are $l = 1$ or $l = 2$ is uncertain since both $l = 1$ and $l = 2$ would appear as double parity states in the SEP spectra.

From the mechanism of rotational l-type doubling for $l = 1$ states [13], we conclude that states 1) and 2) are $l = 2$. Following Jonas' discussion, the splitting between the e and f components of the $l = 1$ states in parity basis is:

$V = \frac{1}{4} q_2 (v_2 + 1) J(J + 1)$

Note that q_2 is positive for HCP which means that the e parity state is expected to lie above the f parity state, following the parity basis convention discussed in the previous section. Evaluation of the splitting between the e and f parity basis states leads to the equation for the effective rotational constants for $l = 1$ states:

$B^e_{eff} = B_v + \frac{1}{4} q_2 (v_2 + 1)$

$B^f_{eff} = B_v - \frac{1}{4} q_2 (v_2 + 1).$

So we obtain

$\Delta B_{eff} = \frac{1}{2} q_2 (v_2 + 1)$

In the case of the (0, 38, 0) state, we fix the value of q_2 as the fitted value of the Franck-Condon bright (0, 38, 0) state: $q_2 = 1.3 \times 10^{-3}$ cm^{-1}. Assuming that $v_2 \approx 30$, we predict that the difference between $l = 1$ e and f parity states would be around $\Delta B = 0.02 \text{cm}^{-1}$

However the observed difference between the B-value of the e and f parity pairs of states 1) and 2) is less than 0.01 cm^{-1} which is much smaller than the expected B-value difference of an unperturbed $l = 1$ pair. Thus we began the fit by assuming

that states 1) and 2) are $l = 2$ states. Looking carefully in the reduced term value plots, one can see that states 1) and 3), 2) and 4) form two pairs of $l = 0$ and 2 states, very similar to the behavior of the main state (0, 38, 0). Following the tentative l assignment for states 1) and 2), the effective Hamiltonian matrix can be expressed as:

e block:

$$\begin{pmatrix} H_{11} & 0 & H_{13} & 0 & H_{15} & 0 \\ 0 & H_{22} & 0 & H_{24} & H_{25} & 0 \\ H_{31} & 0 & H_{33} & 0 & 0 & H_{64} \\ 0 & H_{42} & 0 & H_{44} & 0 & H_{46} \\ H_{51} & H_{52} & 0 & 0 & H_{l=2,m} & H_{l-res} \\ 0 & 0 & H_{63} & H_{64} & H_{l-res} & H_{l=0,m} \end{pmatrix} \tag{2.6}$$

f block:

$$\begin{pmatrix} H_{11} & 0 & H_{13} \\ 0 & H_{22} & H_{23} \\ H_{31} & H_{32} & H^{f}_{l=2,m} \end{pmatrix} \tag{2.7}$$

Note that:

1) There is no interaction between e and f blocks.

2) There is no interaction between the perturbing states with the exception of the interactions between each pair: 1) and 3), 2) and 4).

3) For $l = 0$ states, we have Fermi resonances between $l = 0$ main and both states 3) and 4); For $l = 2$ states, we have Fermi resonances between $l = 2$ main and both states 1) and 2).

It is obvious that the model assumed here is fairly complicated, but the result of the fit was not satisfactory. First, the differences between the calculated and the observed energy levels are significantly larger than experimental error, especially for the perturbing states. Second, if the l-assignment is correct, a J-independent Fermi

resonance mechanism is implied. This means that the intensity of the perturbing states will not increase with J because the off-diagonal matrix elements are constant but the energy difference between the Franck-Condon bright state and the perturbing states increases proportionally with $J(J+1)$. But in the observed SEP spectrum, the intensity ratio of the perturbing states relative to the main state is observed to have no siginificant J dependence.

So the failure of this model forced us to reconsider the $l = 2$ assignment for states 1) and 2). Another possible assignment is $l = 1$. We tried to fit the spectra the same way as before except by replacing the off-diagonal matrix elements of the Fermi resonance by the J-dependent Coriolis interaction between (0, 38, 0) state and the states 1) , 2). It turned out that the fit was still unsatisfactory. The fit results for both models are given in Table 2.2.

State	ν_0	g_{ll}	B_v
$l = 0$ main	23150.71(15)		0.6782(46)
$l = 2$ main	23150.71(15)	7.28(13)	0.6547(54)
$l = 1$ (1)	23143.19(15)	11.67(29)	0.7114(52)
$l = 1$ (2)	23163.21(10)	3.25(14)	0.6541(75)
$l = 0$ (3)	23144.66(12)		0.6735(67)
$l = 0$ (4)	23163.84(64)		0.7035(54)

Table 2.2a. The Least-Square Fit results for HCP (0,38,0) state (in cm^{-1}, 1σ uncertainties in parentheses). We assume that states 1) and 2) are $l = 1$ states. D is assumed to be the same for all states.

State	ν_0	g_{ll}	B_v
$l = 0$ main	23148.76(24)		0.6936(11)
$l = 2$ main	23148.76(24)	7.61(31)	0.6542(14)
$l = 2$ (1)	23147.90(15)	10.84(30)	0.7123(85)
$l = 2$ (2)	23163.17(95)	3.65(3)	0.6542(12)
$l = 0$ (3)	23147.90(15)		0.6724(10)
$l = 0$ (4)	23163.17(95)		0.6726(11)

Table 2.2b. The Least-Square Fit results for HCP (0,38,0) state (in cm^{-1}, 1σ uncertainties in parentheses). We assume that states 1) and 2) are $l = 1$ states. D isassumed to be the same for all states.

It seems that the partial deperturbation of the (0, 38, 0) state has not been successful. We discuss the possible reasons as the following:

1) Since the experiments were aimed at the bending overtones, the energy region covered in the experiments was too restricted around the predicted region of the bending overtone. This led to the possiblity of not observing some of the important perturbing states. So the fit model excluding those states would not be adequate.

2) At an energy as high as 23000cm^{-1}, very close to the calculated energy barrier of the HCP $\leftrightarrow$ HPC isomerization, it is possible that the vibrational wavefunctions of HCP mix with those of HPC. If that happens, the fit only considering the HCP wavefunctions would not give a satisfactory result.

The local depertubation of the HCP (0, 38, 0) state was unsuccessful. More experiments are needed to cover continuously the high energy region above 16000cm^{-1} in order to observe all the possible states. Using the $\tilde{C}$ state as the intermediate would yield more reliable results because the $\tilde{C}$ state appeared to show no Franck-Condon selectivity.

2.8 (0, 40, 0) and (0, 42, 0) States

The PUMP transitions used for the (0, 40, 0) state were Q branch lines of the $\tilde{A}(0,3^1,3)$ band, $J = 4,5,6,10,11,12$. For (0, 42, 0), the PUMP transitions were: $\tilde{A}(0,3^1,3)$ band, $J = 4,5,6,7,8,9,10,11,12,13,14,15$. The observed spectra are fairly complicated and only the Franck-Condon bright states (0, 40, 0) and (0, 42, 0) are fitted to get the spectroscopic constants for the two states.

(v_1, v_2, v_3)	ν_0	g_{22}	B_0	$\gamma_{ll} \times 10^4$	$D \times 10^6$	$q \times 10^4$
(0,2,0)	1334.9812(6)	5.0442	0.6671205(24)	0.058(15)	0.6960(18)	2.322(37)
(0,26,0)	16318.692(3)	5.522(1)	0.65248(9)	-1.01(18)	0.1(7)	1.934(31)
(0,28,0)	17489.333(8)	5.585(2)	0.65104(26)	-1.17(40)	5.2(14)	1.915(49)
(0,30,0)	18648.087(6)	5.651(2)	0.64812(16)	-1.22(25)	1.3(9)	1.892(29)
(0,32,0)[1]	19794.389(4)		0.64632(26)			
(0,34,0)	20928.288(13)	5.857(3)	0.64532(16)	-15.2(13)	4.6(5)	1.810(13)
(0,36,0)	22048.30(17)	6.26(4)	0.6508(20)	-59.1(101)	13.7(52)	1.999(79)
(0,38,0)[2]	23150.71(15)	7.28(13)	0.6782(46)	-121(43)	106(28)	1.3(45)
(0,40,0)[2]	24235.94(21)	8.32(5)	0.722(5)	-246(30)	129(27)	2.6(5)
(0,42,0)[3]	25315.302(30)		0.6915(7)		78(3)	
(0,24,1)	16224.149(4)	5.536(1)	0.65158(8)	-1.37(14)	2.0(5)	1.928(24)
(0,26,1)	17389.563(4)	5.588(2)	0.64945(19)	-1.67(28)	2.0(10)	1.814(39)

Table 2.3. The Spectroscopic Constants of highly vibrationally excited HCP $X^1\Sigma^+$ (in cm^{-1}, 1σ uncertainties in parentheses). D is assumed to be the same for both l=0 and 2 states.

1. Heavily perturbed, only fit to l=0 states.
2. Partially deperturbed.
3. Only l=0 states were observed.

Chapter 3

Cyanogen ↔ Isocyanogen Isomerization

3.1 Introduction

Cyanogen, NCCN, is a linear symmetric molecule. It was first synthesized in 1815. Through the IR spectrum recorded by Moller [16] and the Raman spectrum recorded by Weber [17], the ground state ($\tilde{X}^1\Sigma_g^+$) has been well characterized. Belonging to the point group $D_{\infty h}$, Cyanogen has five normal vibrations, two of which are doubly degenerate bending vibrations. The following table shows the symmetry and frrequency of each vibration:

	symmetry	frequency (cm^{-1})
ν_1, sym CN	Σ_g^+	2324
ν_2, sym CC	Σ_g^+	845
ν_3, anti-sym CN	Σ_u^+	2158
ν_4, *trans*-bending	Π_g	503
ν_5, *cis*-bending	Π_u	233

Table 3.1. Normal mode structure of Cyanogen NCCN.

Several excited electronic states have also been extensively studied. In 1937, Woo *et al* [18] first observed the weak $\tilde{a}^3\Sigma_u^+ \leftarrow \tilde{X}^1\Sigma_g^+$ transition, which was later

confirmed by Callomon *et al* [19]. It was found that the excited $\tilde{a}^3\Sigma_u^+$ state is linear and the origin of the $\tilde{a} \leftarrow \tilde{X}$ transition is at $\sim$ 300 nm. Another weak electronic transition, $\tilde{b}^3\Delta_u \leftarrow \tilde{X}^1\Sigma_g^+$, was observed around 250 nm by Cartwright *et al* [20] at high resolution. The $\tilde{b}^3\Delta_u$ electronic state is also linear. These two transitions arise from the $\pi_g^* \leftarrow \pi_u$ excitation and they are weak because they are spin forbidden triplet-singlet transitions made weakly allowed by spin-orbit interaction. The strong singlet-singlet $\pi_g^* \leftarrow \pi_u$ transitions were observed by Woo *et al* [21] in 1932 and Bell *et al* [22] in 1969. They identified the linear-linear transitions of $\tilde{A}^1\Sigma_u^- \leftarrow \tilde{X}^1\Sigma_g^+$ and $\tilde{B}^1\Delta_u \leftarrow \tilde{X}^1\Sigma_g^+$ at 220 nm and 207 nm, respectively. Absorption intensities were found to be 10^4 times stronger than those of the triplet-singlet transitions. Cyanogen also has a strong electronic transition in the vacuum ultraviolet region near 170 nm, and the upper state has been assigned to be $\tilde{C}^1\Pi_u$ arising from a $\pi^* \leftarrow n$ excitation. The symmetry-forbidden transitions of $\tilde{A}^1\Sigma_u^- \leftarrow \tilde{X}^1\Sigma_g^+$ and $\tilde{B}^1\Delta_u \leftarrow \tilde{X}^1\Sigma_g^+$ are induced by vibronic coupling involving mode 4.

One interesting feature about the Cyanogen molecule is its isomers Isocyanogen (CNCN) and Diisocyanogen (CNNC) on the ground S_0 surface. *Ab initio* calculations [23] show that the isomers are separated by energy barriers. As shown in Figure 3.1, the lowest energy barrier starting from NCCN is the transition state to CNCN at $\sim$ 23150 cm^{-1}. CNCN and CNNC have been synthesized by Stroth [24] and Yamada [25], respectively. Through the IR and Raman spectra, they concluded that both CNCN and CNNC are linear in the ground state and are fairly stable in the gas phase. In our group, there has been a lot of experimental effort invested in the study of unimolecular isomerization, such as acytelene $\rightarrow$ vinidylene, and HCP $\rightarrow$ HPC. But a big problem in the above two systems is that the higher energy isomer there is exteremely short-lived and not well understood. Also, the vibrational energy sifficient to surmount the barrier is at least 15,000 cm^{-1} for acetylene and 24000 cm^{-1} for HCP. Up to date, no experimental data have been observed to indicate whether isomerization might occur in a spectroscopically detectable way.

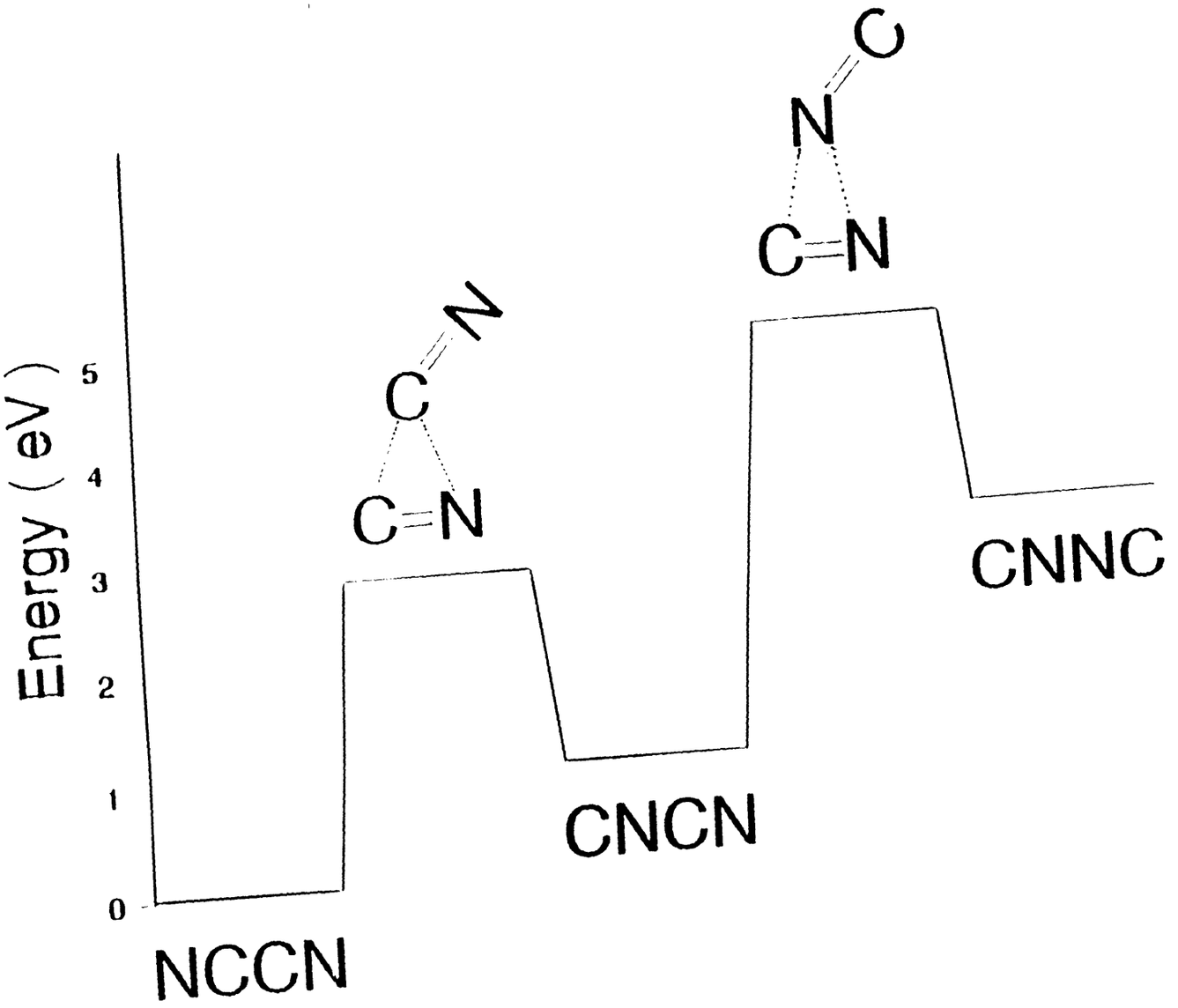

Figure 3.1 C_2N_2 isomers on ground state PES.

The three isomers of $(CN)_2$ present a unique opportunity for studying the unimolecular isomerization process because, first of all, all the isomers have been synthesized and all are fairly stable in the gas phase. The ground state of all three isomers has been studied by Infrared Spectroscopy and this has made it easier to determine whether there would be any spectroscopically recognizable sign of isomerization. On the other hand, if we start from the less stable isomers, CNCN or CNNC, the energy barrier will be much lower than that starting from NCCN. *Ab initio* calculation results show that the barrier from CNCN to NCCN is $\sim$ 14000 cm^{-1}, only about 60% of the barrier of NCCN to CNCN.

Following the above discussion, we propose an experiment utilizing a unique feature of the Cyanogen isomers. We plan to start from the molecule Isocyanogen and excite the Isocyanogen molecule to highly vibrationally excited levels of the ground state using the techinque of Stimulated Emission Pumping. In the following sections, we discuss in detail the proposed experimental study of CNCN $\rightarrow$ NCCN isomerization. The crucial question is whether CNCN has a low-lying bent electronic state so that we can excite the CNCN molecule to its excited electronic state and then DUMP the molecule to highly vibrationally excited levels on the ground electronic state of CNCN, so that isomerization to NCCN might affect the Franck-Condon accessible vibrational levels. The bent geometry of the excited state is important because it ensures favorable Franck-Condon overlaps with the high vibrational levels of the ground state.

3.2 *Ab initio* Calculation Results

3.2.1 Molecular Orbital Analysis

Isocyanogen is linear in the ground electronic state with the symmetry of $C_{\infty v}$ and has the configuration of $(1a_1)^2(2a_1)^2(3a_1)^2(4a_1)^2(5a_1)^2(6a_1)^2(7a_1)^2(8a_1)^2(9a_1)^2(1\pi)^4(2\pi)^4$. The HOMO and LUMO of the CNCN molecule are $1\pi 2\pi$ and $3\pi 4\pi$, respectively. Obviously, we would expect that the lowest excited electronic state would correspond to

the $3\pi \leftarrow 2\pi$ excitation. We want to know whether there is a bent excited electronic state.

The Walsh diagram for CNCN is shown in Figure 3.2. Let us consider the trans-bend motion first. From the linear $\leftrightarrow$ trans-bend Walsh diagram, one would expect that if there is an electron excited from the 2π to the 3π orbital, there are 4 possible excitations: $a'' \leftarrow a''$, $a'' \leftarrow a'$, $a' \leftarrow a''$, and $a' \leftarrow a''$. Note that from the selection rules for electronic dipole transitions, only the $a' \leftarrow a''$ and $a'' \leftarrow a'$ excitations are allowed. If the excitation is from $a' \leftarrow a''$, we can see from the Walsh diagram, that the a' orbital would strongly prefer the bent geometry, while the a'' orbital will be somewhat indifferent between the linear and the bent structures. The curvature of the Walsh diagram can be explained by the nodal character of the π orbitals of CNCN in Figure 3.3. For example, for 3π orbital, the a' orbital component lies in the molecular plane. The in-plane trans-bend displacement of the atoms from the linear structure will decrease the anti-bonding effect between the π orbitals and increase the bonding effect between the π orbitals. This will decrease the total energy of the molecule, hence it will make the molecule more stable. The other a'' orbital lies perpendicular to the molecular plane. It is obvious that an out-of-plane trans-bend displacement of the atoms would have little effect on the bonding character of the π orbitals, so the Walsh diagram for the a'' orbital is close to a straight line. Altogether, the larger the trans-bent angle, the more stable the excited electronic state will be. So we expect that there will be a $^1A''$ trans-bent excited state.

With the above qualitative analysis, we only predict that a trans-bent structure will be favorable for one of several possible excitations. But we don't know the exact energy of the corresponding excited state. Since the dissociation energy of Cyanogen is $\sim$ 47000 cm^{-1} and from the *ab initio* calculation for Cyanogen and Isocyanogen, we know that Isocyanogen lies about 9000 cm^{-1} above Cyanogen on the ground state PES, this raises an important question: even if there is a bent excited state for CNCN, is its minimum below or above the adiabatic dissociation limit? If it is above the dissociation limit and its lifetime is therefore much shorter than the 10ns range, it will not be suitable as an intermediate state in our SEP experiments. On the other

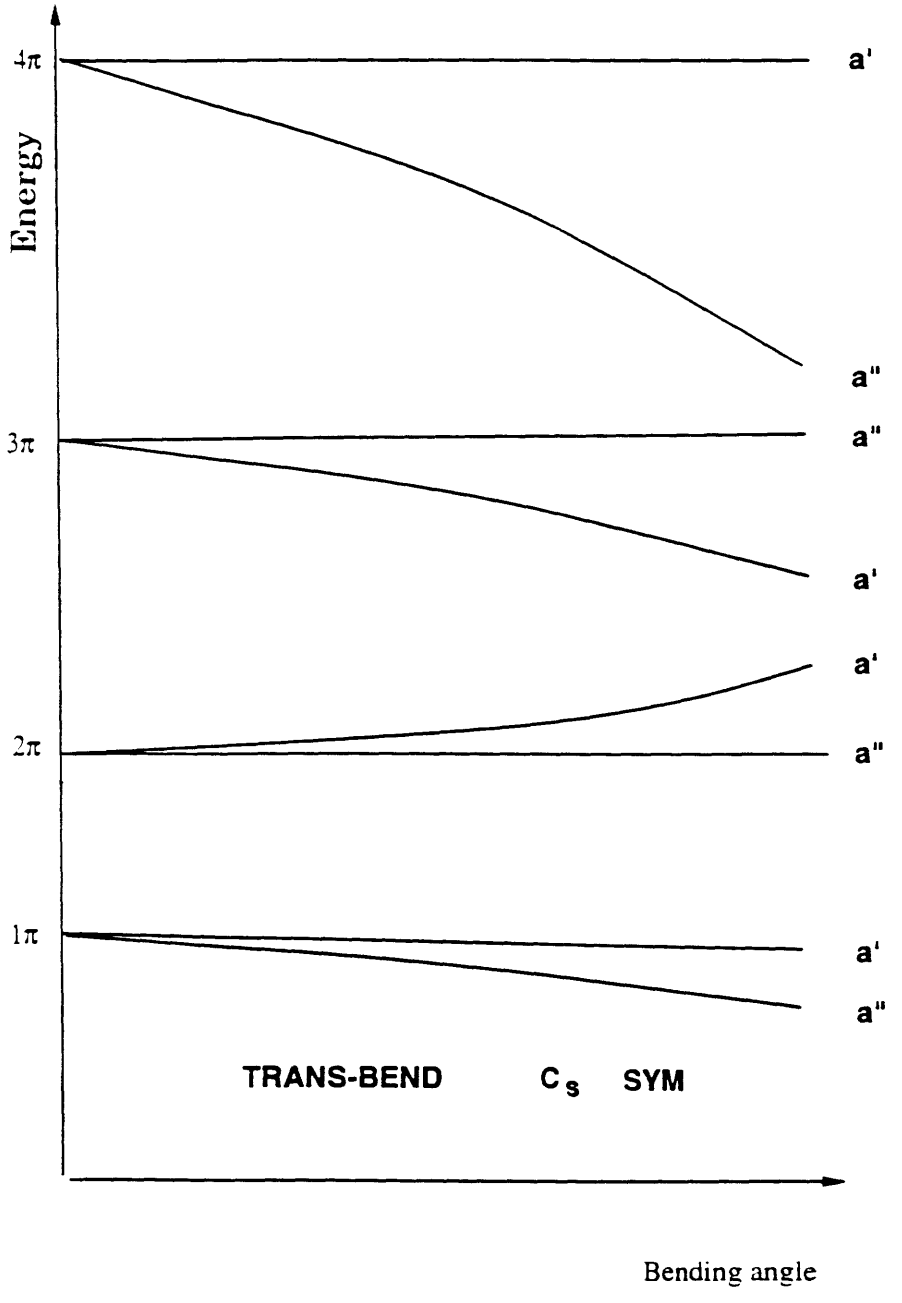

Figure 3.2 Walsh diagram for CNCN

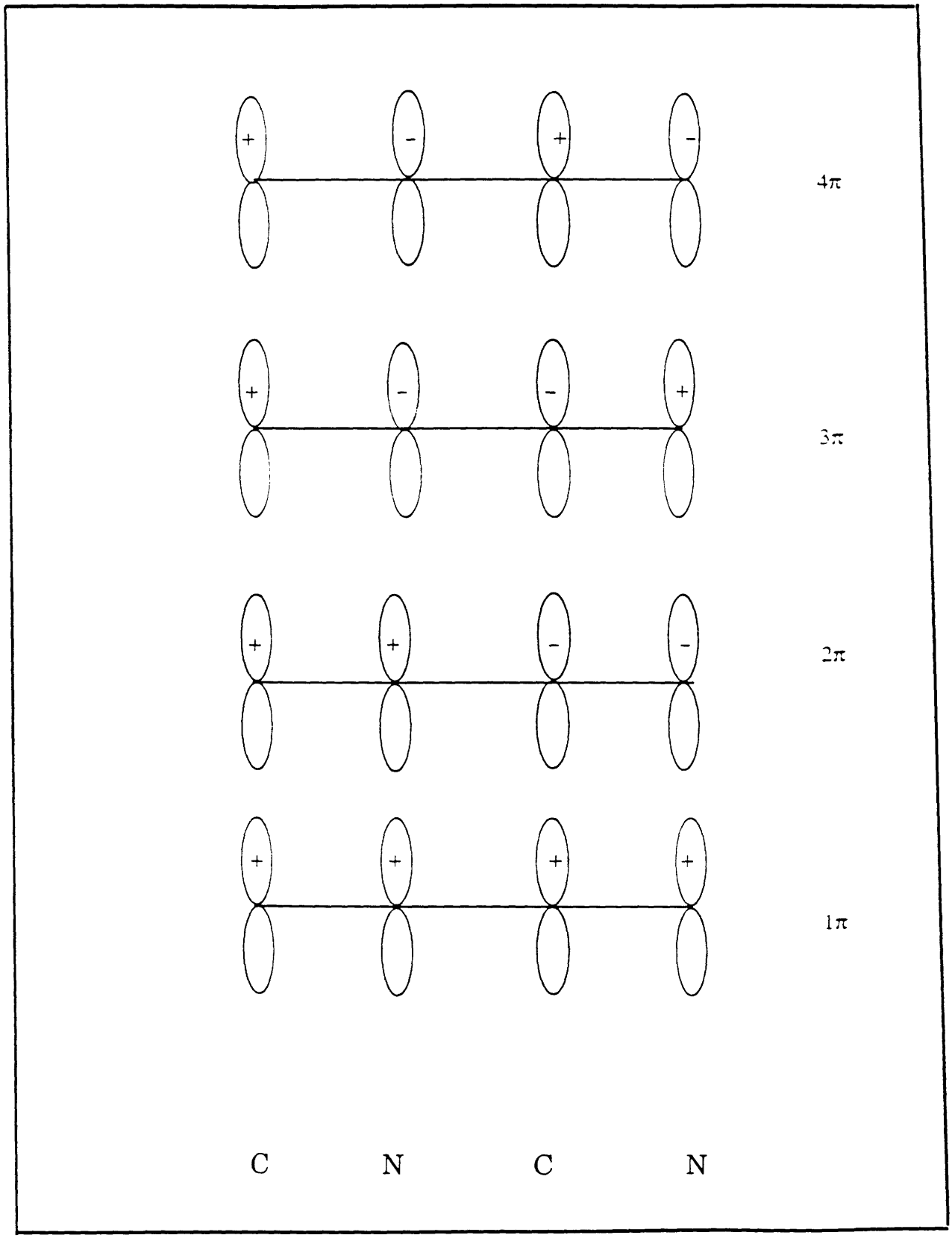

Figure 3.3 Nodal character of the π orbitals of CNCN

hand, if the excited state lies below the dissociation limit, this will be very favorable for the SEP experiments, since there will be good Franck-Condon overlap between the bent state and the high vibrational levels of the trans bending normal mode. All these questions must be answered by theoretical calculations.

3.2.2 *Ab initio* results

Sherrill and Schaefer [26] performed CISD calculations for the $\tilde{A}^1A''$ state of Isocyanogen and their results will be briefly discussed in the following.

Indeed, the calculation shows that there is a bent $^1A''$ state that arise primarily from the $3\pi \leftarrow 2\pi$ excitation. They initially found two minima at the SCF level of calculation. But at the CISD level, the two SCF minima converged to the same structure as shown in Figure 3.4. They estimated that $^1A''$ state lies about 41100 cm^{-1} (T_e) above the CNCN ground electronic state. Sherrill and Schaefer also calculated the harmonic vibrational frequencies for the five normal vibrations listed in Table 3.2, except for the mode arising from the torsional motion. Note that the calculated energy of the A'' state is 2000 cm^{-1} above the lowest energy dissociation limit, taking into account that CNCN lies 9000 cm^{-1} above NCCN.

	SCF	CISD
$\omega_1(C_2 - N_2)$	2151	1977
$\omega_2(N_1 - C_2)$	814	1331
$\omega_3(C_1 - N_1)$	1205	1051
$\omega_4(N_1 - C_2 - N_2)$	663	650
$\omega_5(C_1 - N_1 - C_2)$	270	222
$\omega_6(torsion)$	457	(457)

Table 3.2. Harmonic Vibrational Frequencies (cm^{-1}) of the CNCN $\tilde{A}^1A''$ state. The result is from the calculation at the TZ2P level, except that the value for the torsion is from results at the level of SCF-DZP.

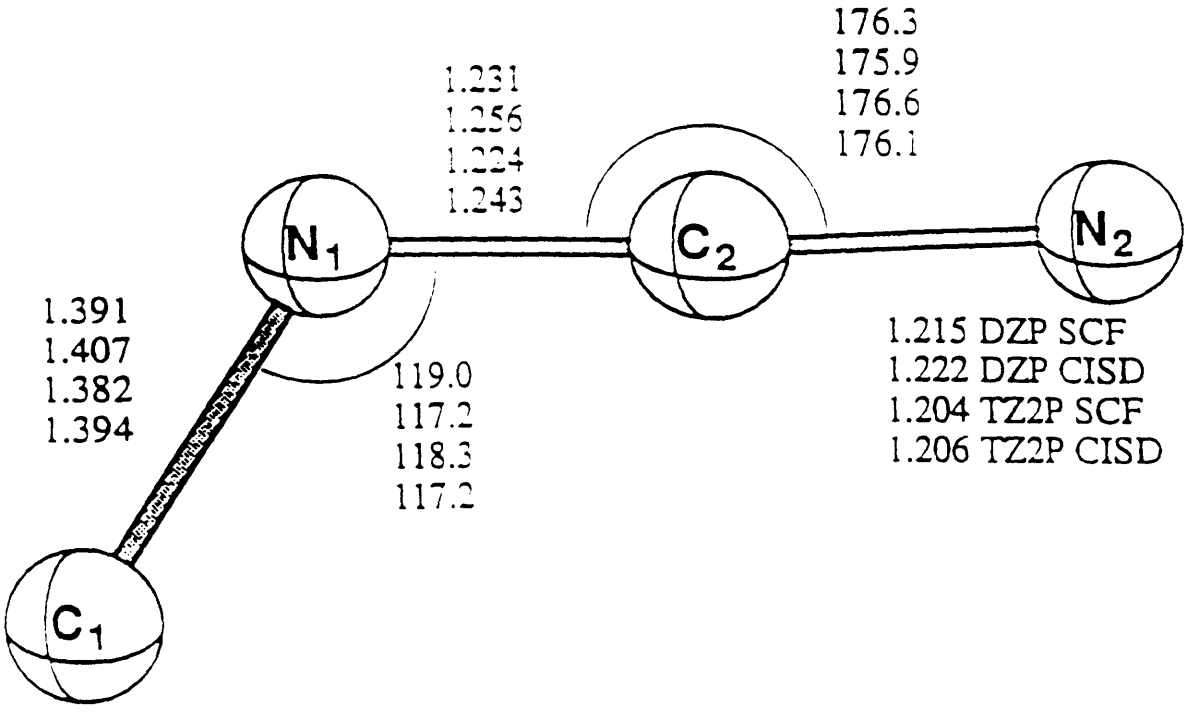

Figure 3.4 $^1A''$ state structure of CNCN.

3.2.3 Discussion

The calculation confirmed our expectation that there is a bent $^1A''$ state for Isocyanogen. But it also showed that the $^1A''$ state lies above the lowest dissociation limit to $CNX^2\Sigma^+ + CNX^2\Sigma^+$. The remaining question is whether the $^1A''$ state is sufficiently stable to be used as an intermediate state in the SEP experiments.

The fact that all six normal mode frequencies are real at the DZP SCF level from Sherrill and Schaefer's calculation indicates that the calculated $^1A''$ state is a true minimum on the potential energy surface at the level of their calculation. At higher levels of calculation, they were able to compute five real frequencies but not the out of plane torsion. But there is no reason to believe that the vibrational frequency of the torsion would become imaginary at higher levels of calculation. This is a strong indication that the $^1A''$ state would be stable at the origin.

Sherrill and Schaefer also tried to calculate the dissociation barrier of the CNCN $^1A''$ state, but they were unable to determine the barrier height. Note that the $^1A''$ state of CNCN can only dissociate to CN $X^2\Sigma^+$ and $A^2\Pi$ states. It was estimated that the dissociation barrier of $^1A''$ CNCN $\rightarrow$ CN $X^2\Sigma^+$ + CN $A^2\Pi$ to be $\sim$ 7000 cm^{-1}. So the low vibrational levels of $^1A'$ CNCN will be below the dissociation energy barrier of the channel: $^1A''$ CNCN $\rightarrow$ CN $X^2\Sigma^+$ + CN $A^2\Pi$.

It is possible that the $^1A''$ state of CNCN can be predissociated by a state which dissociates adiabatically into two CN $X^2\Sigma^+$ fragments. From symmetry, two CN $X^2\Sigma^+$ states correspond to one singlet state $^1A'$ and one triplet state $^3A'$ of CNCN. The only possible predissociation mechanism would be for the $^1A''$ state of CNCN to interact with a triplet state $^3A'$ and dissociate along the triplet surface. The interaction between the singlet and the triplet would necessarily be a spin-orbit interaction.

There have been no reports on the triplet states of Isocyanogen in the literature and the calculations of Sherrill and Schaefer are to our knowledge, the first to deal with the excited electronic states of CNCN. Knowing nothing about the lowest triplet surface of CNCN, we cannot say anything about the possible spin-orbit interaction bewteen a singlet state and a triplet state. However, we can conclude that the bent $^1A''$ state of CNCN could possibily predissoicate to two CN $X^2\Sigma^+$ fragments only

through a spin-orbit interaction with the triplet state $^3A'$.

3.3 Conclusion

We predicted the existence of a low-lying bent $^1A''$ state of CNCN and this prediction was confirmed by the *ab initio* calculation by Sherrill and Schaefer. The bent $^1A''$ state of CNCN is found to lie 2000 cm^{-1} above the lowest dissociation limit. The calculation shows that the vibrational frequencies of the CNCN $^1A''$ state are all real and this implies that the $^1A''$ state is a true minimum on the potential energy surface. As for the possibility of dissociation into two ground state $X^2\Sigma^+$ CN fragments, direct dissociation is impossible since the origin of $^1A''$ state is 7000 cm^{-1} below the lowest possible CN $X^2\Sigma^+$ + CN $A^2\Pi$ asymptote. Predissociation by the $^3A'$ state is a possibility, but without more detailed calculation, it is impossible to estimate the predissociation lifetime of CNCN. But the results so far indicate that the $^1A''$ state of CNCN will be suitable as an SEP intermidiate.

The bent $^1A''$ state of CNCN is ideally suited to the proposed SEP experiments to probe the CNCN $\leftrightarrow$ NCCN isomerization. From the structure shown in Figure 3.2, we would expect all the vibrational modes of the $\tilde{X}^1\Sigma^+$ state to be Franck-Condon active with respect to the $^1A''$ state of CNCN. Combining the advantage of lower energy barrier from CNCN to NCCN and the powerful technique of SEP, we expect that the SEP experiments on CNCN $\rightarrow$ NCCN isomerization would be very likely to succeed.

Bibliography

[1] T. E. Gier. J. Am. Chem. Soc. **83**, 1769(1961).

[2] J. W. Johns, H. F. Shurvell, and J. K. Tyler, Can. J. Phys. **47**, 893(1969).

[3] S. P. Karna, P. J. Bruna, and F. Grein, Can. J. Phys. **68**, 499(1990).

[4] X. Liu and J. N. Murrell, J. Chem. Soc.Farady Trans. **88**, 1503(1992).

[5] K. K. Lehmann, S. C. Ross, and L. L. Lohr, I. Chem. Phys. **82**, 4460(1985).

[6] M.T. Nguyen and T.-K. Ha, J. Mol. Struc. THEOCHEM **139**, 145(1986).

[7] N. L. Ma, S. Wong, M. Paddon-Row, and W.-K. Li, Chem. Phys. Lett. **213**, 189(1993).

[8] C. E. Hamilton, J. L. Kinsey and R. W. Field, Annu. Rev. Phys. Chem. **37**, 493(1986).

[9] M. J. Hopkinson, H. W. Kroto, J. F. Nixon, and N. P. C. Simmons, J. Chem. Soc. Chem. Commun. **1976**, 513.

[10] T. Kavanaugh and K. Yamashita, unpublished results.

[11] Y.-T. Chen, D. M. Watt, and R. W. Field, J. Chem. Phys. **93**, 2149(1990); Y. Chen, Ph.D. thesis, MIT(1988).

[12] E. J. Friedman-Hill, Ph.D. thesis, MIT, 1992.

[13] D. M. Jonas, Ph.D. thesis, MIT, 1992.

[14] D. R. Papousek and M. R. Aliev, *Molecular Vibrational-Rotational Spectroscopy*, Elsevier Scientific Publishing, New York, 1982.

[15] Y.-T. Chen, Y. Ohshima, K.-C. Lin, D. M. Watt, R. J. Silbey, R. W. Field, and K. K. Lehmann, in preparation.

[16] C. K. Moller and B. P. Stoicheff. Can. J. Phys. **32** 635(1954).

[17] I.-Y. Yang and A. Weber, J. Chem. Phys. **67**, 3084(1977).

[18] S.-C. Woo and T.-K. Liu, J. Chem. Phys. **5**, 161(1937).

[19] J. H. Callomon and A. B. Davey, Proc. Phys. Soc. **82**, 335(1963).

[20] G. L. Cartwright, D. O. O'Hare, A. D. Walsh, and P. A. Warsop, J. Mol. Spec. **39**, 393(1971).

[21] S. C. Woo and R. M. Badger, Phys. Rev. **39** 932(1937).

[22] S. Bell, G. L. Cartwright, A. D. Walsh, and P. A. Warsop, J. Mol. Spec. **30**, 162(1969).

[23] K. K. Sunil, J. H. Yates, and K. D. Jordan, Chem. Phys. Lett. **171**, 185(1990); M. T. Ngugen, Chem. Phys. Lett. **157**, 430(1989).

[24] F. Stroh and M. Winnewisser, Chem. Phys. Lett. **155**, 21(1989); F. Stroth B. P. Winnewisser, M. Winnewisser, H. P. Resenauer, G. Maier, S. J. Goede, and F. Bickelhaupt, Chem. Phys. Lett. **160**, 105(1989).

[25] K. M. T. Yamada, M. W. Markus, G. Winnewisser, W. Joentgen, R. Kock, E. Vogel, and H. J. Altenbach, Chem. Phys. Lett. **160**, 113(1989).

[26] C. D. Sherrill and H. F. Schaefer III, private communication.